

# Particle-in-Cell simulations of electron spin effects in plasmas

Gert Brodin,<sup>\*</sup> Amol Holkundkar,<sup>†</sup> and Mattias Marklund<sup>‡</sup>  
*Department of Physics, Umeå University, SE-901 87 Umeå, Sweden*

We have here developed a particle-in-cell code accounting for the magnetic dipole force and for the magnetization currents associated with the electron spin. The electrons is divided into spin-up and spin-down populations relative to the magnetic field, where the magnetic dipole force acts in opposite directions for the two species. To validate the code, we have studied the wakefield generation by an electromagnetic pulse propagating parallel to an external magnetic field. The properties of the generated wakefield is shown to be in good quantitative agreement with previous theoretical results. Generalizations of the code to account for more quantum effects is discussed

PACS numbers: PACS: 52.35.Mw, 52.65.Rr, 03.65.Sq

Recently much work has been devoted to the field of quantum plasmas. Many aspects of the field are well described in books and review papers [1–5]. The interest in the field has been motivated by laboratory applications in for example plasmonics [6, 7], quantum wells [8] and high-density laser plasma interaction [3, 9] as encountered e.g. in inertial confinement fusion (ICF) schemes. Furthermore, astrophysical applications [10] of quantum plasmas has played a role. The theoretical approaches includes quantum kinetic theories such as e.g. the Kadanoff-Baym kinetic [1] or the Wigner equation [2], various quantum hydrodynamic equations [11–13] and spin kinetic theories [14–17]. Due to the complex nature of the governing equations, many problems involving nonlinearities and/or inhomogeneities must be addressed numerically. A successful method applied to *classical plasmas* is the celebrated particle-in-cell (PIC) approach (see e.g. [18–21]). Due to the classicality of the concepts this have had a limited impact to quantum plasmas. It should be noted, however, that the Feynman path integral formulation has been used to develop a PIC treatment [22, 23] that includes particle dispersive effects in a semi-classical fashion. This is computationally costly, and the number of quantum particles that can be included in the code is far less than in the classical case [22, 23].

In our paper we have chosen another approach in order to develop a PIC-code including certain quantum features. We first note that the Wigner equation reduces to the classical Vlasov equation for macroscopic scale lengths longer than the thermal de Broglie wavelength. Hence particle dispersive effects [2, 24] can be neglected on such scales. On the other hand, the physics associated with the electron spin (e.g. the magnetic dipole force and the spin magnetization currents [15–17]) does not vanish for long scale lengths. Hence, in this paper we will aim to develop a PIC code applicable on macroscopic scales, accounting for the magnetic dipole force and the spin magnetization currents. While a classical magnetic dipole moment fits very well into the PIC-concept, it is clear that the difference between a classical magnetic dipole moment and the spin must be acknowledged. The present approach builds on the findings of Ref. [25]. It was then observed that more elaborate models for the spin physics reduces to a simple one for frequencies below the spin precession frequency (which is approximately the same as the cyclotron frequency).

Specifically this meant that for a dynamical time scale slower than the cyclotron frequency, the electrons could be modelled as consisting of two fluids, one with a spin up state relative the magnetic field and one with a spin down state. The two electron species are then subject to magnetic dipole forces acting in opposite directions. A 1D PIC-code based on this concept has been developed, and is tested in the present paper. In particular we let a short electromagnetic (EM) pulse propagate along an external magnetic field in a plasma, and study the wake field induced. Comparing with theoretical results, we find that the PIC-code is able to reproduce previous findings [26, 27].

Due to the classical nature of the PIC-concept, it is theoretically difficult to generalize it to the quantum regime. Although the basic effect of wave particle dispersion (as described by the Schroedinger equation) can be handled to a certain extent (see e.g. Refs. [22, 23]) it is computationally costly. In particular the number of particles needed to capture particle dispersion is increased by a factor of at least a thousand. On the other hand, the effect of particle dispersion is not important for scale lengths much longer than the characteristic de Broglie wavelength [2, 16]. However, other quantum effects may play a role for the long scale dynamics [15–17]. In particular, when  $\mu_B B/k_B T$  or  $\mu_B B/m_i c_A^2$  approaches unity (here  $\mu_B = e\hbar/2m_e$  is the Bohr magneton,  $B$  is a characteristic magnetic field value,  $T$  is a characteristic temperature,  $e$  is the elementary charge,  $\hbar$  is the Planck constant divided by  $2\pi$ ,  $m_e$  and  $m_i$  is the electron and ion mass respectively, and  $c_A$  is the characteristic Alfvén velocity), the magnetic dipole force and the magnetization current associated with the electron spin may become important [15, 28]. To a significant extent, the magnetic dipole force associated with the spin is comparable to a classical magnetic dipole force, and the magnetic moment associated with the magnetic field is comparable to a classical magnetic moment. This means that spin effects can be conceptually straightforward to include in a PIC-scheme. A complication is that unlike a classical magnetic dipole moment, the probability distribution of the spin for a single particle is by necessity spread out (since the different spin components does not commute). This suggests that spin-velocity correlations [29] may affect the dynamics, and that updating the variables using the Heisenberg equation of mo-

tion may be somewhat inaccurate. However, the case where the dynamical time scale is slower than the electron spin precession frequency (which is approximately the same as the electron cyclotron frequency) and the spatial scale is longer than the Larmor radius has been studied by Ref. [25]. It was then deduced that the electrons can be described by a rather simple model, where only two spin states, up and down relative to the magnetic field are needed. The quantum effects then enter as a magnetic dipole force in the equation of motion (in opposite directions for the two spin states, which is described as two different species), and as a magnetization along the magnetic field, which is proportional to the density difference between the spin-up and spin-down electrons.

Based on the concepts described above, we will extend an 1D Particle-In-Cell simulation (LPIC++) (see Ref. [21]) in order to incorporate the effect of up- and down spin states in the governing dynamics. In this model the ions are treated as a classical particles. However the electrons come in two different species, one with spin up and the other with spin down. The presence of an external magnetic field along the direction of laser propagation is also included in the model. The governing equations for particle motion with two electron species will now read as,

$$m_e \frac{d\mathbf{v}_\downarrow}{dt} = q_e(\mathbf{E} + \mathbf{v}_\downarrow \times \mathbf{B}) - \mu_B \nabla B \quad (1)$$

$$m_e \frac{d\mathbf{v}_\uparrow}{dt} = q_e(\mathbf{E} + \mathbf{v}_\uparrow \times \mathbf{B}) + \mu_B \nabla B \quad (2)$$

where the arrows indicate the different spin states and  $B$  is the magnitude of the magnetic field. Moreover Ampere's law is written as,

$$\nabla \times (\mathbf{B} - \mu_0 \mathbf{M}) = \mu_0 \mathbf{j}_f + \frac{1}{c^2} \frac{\partial \mathbf{E}}{\partial t} \quad (3)$$

where the free current including the ions is  $\mathbf{j}_f = q_e(n_\downarrow \mathbf{v}_\downarrow + n_\uparrow \mathbf{v}_\uparrow) + q_i \mathbf{v}_i$ , and the magnetization due to spin is  $\mathbf{M} = \mu_B \mathbf{b}(n_\downarrow - n_\uparrow)$ , where  $\mathbf{b}$  is the unit vector in the direction of magnetic field, i.e.  $\mathbf{b} = \mathbf{B}/B$ . Two assumptions is necessary for this model to hold

i) That the spin-relaxation time is longer than the time scales of study. Otherwise the two spin-states cannot be treated as independent fluids.

ii) That the time scale of study is longer than the spin precession time scale. Otherwise the spin vector (and the magnetic moment) will not necessarily point in the direction of the magnetic field.

Before we start the studies it is convenient to rewrite the equations in dimensionless form. We use the inverse laser frequency  $\omega^{-1}$  to normalize time (i.e. the normalized time  $t_n$  is  $t_n = \omega t$ ),  $c/\omega$  to normalize distance, the normalized spin-down (up) density is  $n_{n\downarrow(\uparrow)} = (n_{\downarrow(\uparrow)} e^2 / \epsilon_0 m) / \omega^2$ , and the dimensionless electric and magnetic field are  $\mathbf{E}_n = e\mathbf{E}/m_e \omega c$  and  $\mathbf{B}_n = e\mathbf{B}/m_e \omega$ , respectively. Dividing the magnetic field

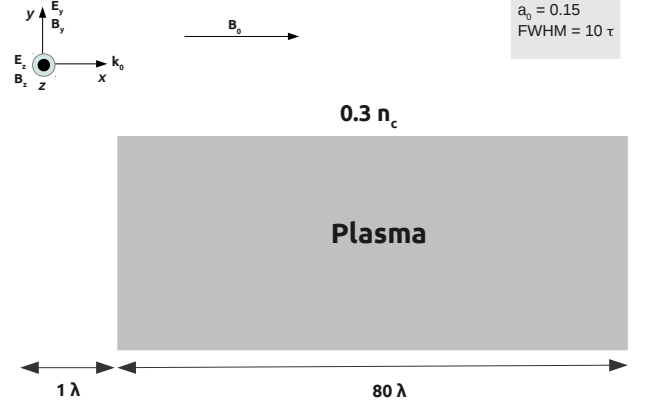


FIG. 1. Simulation geometry of the problem.

into a homogeneous static field  $B_0 = B_0 \hat{\mathbf{x}}$  and a dynamic magnetic field, the basic equations in normalized form becomes

$$\frac{d\mathbf{v}_\downarrow}{dt_n} = \mathbf{E} + \mathbf{v}_\downarrow \times \left( \mathbf{B} - \frac{\omega_c}{\omega} \hat{\mathbf{x}} \right) - \frac{\hbar \omega}{mc^2} \nabla B \quad (4)$$

$$\frac{d\mathbf{v}_\uparrow}{dt_n} = \mathbf{E} + \mathbf{v}_\uparrow \times \left( \mathbf{B} - \frac{\omega_c}{\omega} \hat{\mathbf{x}} \right) + \frac{\hbar \omega}{mc^2} \nabla B \quad (5)$$

and

$$\nabla \times \left( \mathbf{B} - \frac{\hbar \omega}{mc^2} \mathbf{b}(n_\downarrow - n_\uparrow) \right) = (n_\downarrow \mathbf{v}_\downarrow + n_\uparrow \mathbf{v}_\uparrow) + \frac{\partial \mathbf{E}}{\partial t} \quad (6)$$

Here for notational convenience the subscript  $n$  denoting normalized quantities have been omitted on all variables and operators. The term  $(\omega_c/\omega)\mathbf{x}$ , where  $\omega_c = eB_0/m$  represents the constant static part of the magnetic field, and hence  $\mathbf{B}$  is the dynamic part only. Consequently we have  $B = |(\omega_c/\omega)\mathbf{x} + \mathbf{B}|$ . For all simulations presented below the dimensionless parameter  $\hbar\omega/mc^2$  is chosen to be  $\hbar\omega/mc^2 = 2\pi \times 10^{-4}$ . The typical simulation geometry for the problem is shown in Fig. 1. For all the results presented here the normalized electric field amplitude is considered as 0.15. The circularly polarized laser with FWHM duration of 10 period times propagates through the plasma along the x direction. The external magnetic field is considered along the x direction with amplitude in dimensionless unit ( $b_0 = eB_0/m_e \omega$ ). With these parameters the characteristic velocities of the problem (e.g. phase velocity and group velocity) will be of the order of  $c$ . The thermal velocity is considered to be much smaller than this, and hence the temperature is effectively zero in our simulations. Finally, the plasma of length 80 wavelengths is taken to have the total unperturbed electron density of  $n_\downarrow + n_\uparrow = 0.3$  (Fig. 1).

In Fig. 2 the density perturbation of the electrons with spin-up and with spin-down is shown after the passage of a circularly polarized EM wave. As can be seen the density perturbations of the two species of electrons are almost

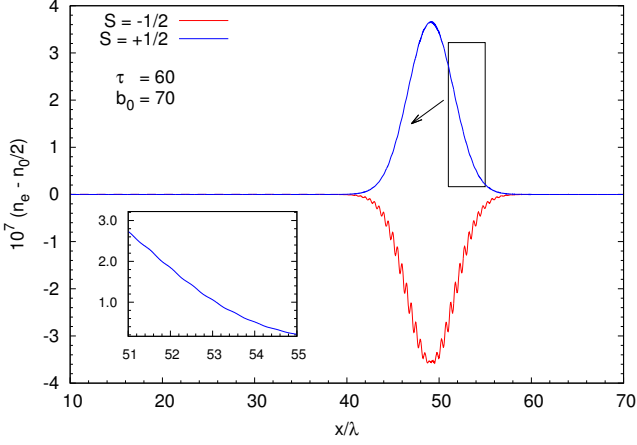


FIG. 2. Density perturbation with respect to unperturbed density for electron species with spin  $+1/2$  and  $-1/2$  are presented at  $60\tau$  with external magnetic field  $b_0 = 70$ . Inset shows the magnified version of the  $+1/2$  spin state plot, where the presence of the small second harmonic component can be seen.

opposite. This is also clear from Fig. 3, where the total (spin-up + spin-down) density perturbation is shown, which is smaller than the individual density perturbations of the up- and down- species by roughly a factor 20. Furthermore, we see that the total density perturbation has a rapidly oscillating second harmonic component which is of the same order of magnitude as the low-frequency component. Since the electromagnetic wave is circularly polarized, we note that the second harmonic components are associated with the discrete particle (collisional) effects of the PIC-code. To understand the results in more detail, we first note that the spin properties in the given geometry only enters nonlinearly. Since the magnetic field perturbation is purely transverse, we note that  $\nabla B = \nabla \sqrt{B_0^2 + B_\perp^2} \approx (1/2)\nabla(B_\perp^2/B_0)$ , including only up to second order nonlinearities in the transverse wave magnetic

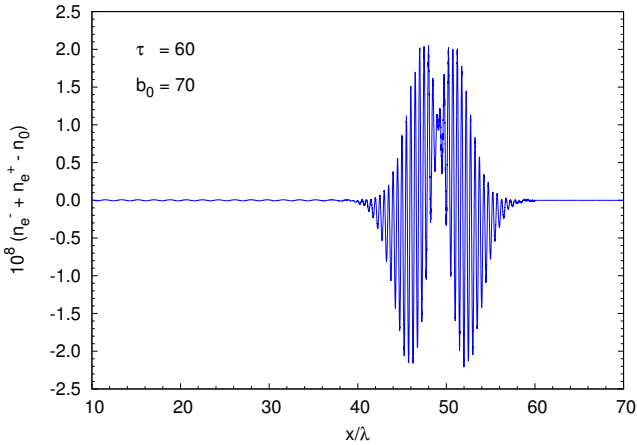


FIG. 3. Spatial profile of total electron density at  $60\tau$  for the external magnetic field  $b_0 = 70$ .

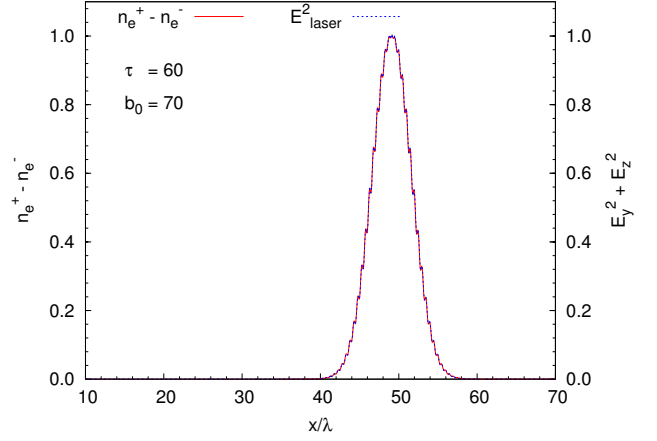


FIG. 4. Electron density response to the electric field of circularly polarized laser pulse is presented. Both electric field and difference between electron densities of both species are normalized to unity. It should be noted that both curve are identical and it is not possible to distinguish one from another in this figure.

field  $B_\perp$ . The spin dependent part of the perturbation is then induced by the magnetic dipole force, which is directed in opposite directions for the spin-up and down species.

In order to verify the interpretation that the density difference between the up- and down electron species comes is a direct response to the magnetic dipole force of the wave field, we compare the profile of  $|\mathbf{E}|^2$  (which is proportional to  $B_\perp^2$ ) with that of the density difference  $n_e^+ - n_e^-$ . The result is shown in Fig. 4. It turns out that the matching is so accurate that two separate curves cannot be recognized, as they are fully overlapping.

Next our aim is to make a quantitative comparison of the output from the PIC-code with analytical results derived by Ref. [27]. Eqs. (19) and (20) together with Eq. (20) of Ref. [27] show that for strong magnetic fields ( $\omega \ll \omega_c$ ) the peak electric amplitude of the wakefield scales as

$$E_{\text{peak}} \propto \frac{c_1(n_{0+} - n_{0-})}{B_0} + \frac{c_2}{B_0^2}$$

where  $c_1$  and  $c_2$  are constants. Fitting the peak amplitude as a function of the magnetic field as calculated from the PIC-code, with a curve of this type, a good agreement is found, as shown in Fig. 5. Specifically three different cases are investigated. A pure spin up state, a pure spin down state and a mixed state with  $n_{0+} = n_{0-}$ . The constant  $c_1$  varies less than 0.2% between the three cases, whereas  $c_2$  varies slightly from  $5.735 \times 10^{-4}$  to  $5.328 \times 10^{-4}$  when switching from a pure spin-up plasma to a spin down plasma.

Another interesting variable to study is the spin polarization induced by the EM wave for an plasma with equal number of particles in the spin up and the spin down states initially. The spin polarization is monitored by plotting the peak of the density difference  $n_+ - n_-$ , which is also closely related to the spin induced magnetization. According to the theory (see e.g.

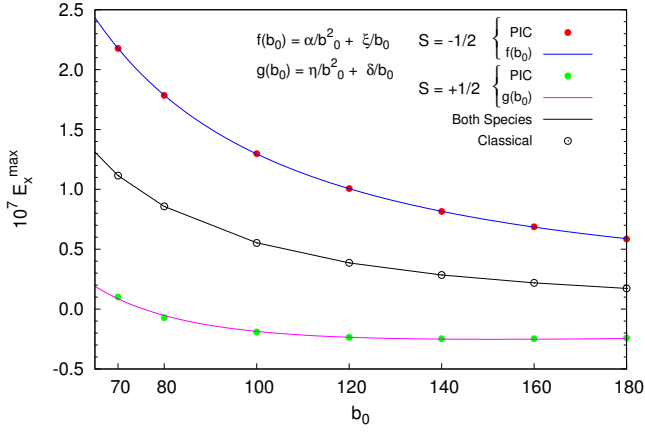


FIG. 5. Maximum amplitude of wakefield at  $60\tau$  is presented by varying the magnitude of external magnetic for electrons species with different spin states. For all the plasma electrons with spin down states (red circles) the associated function  $f(b_0)$  is fitted (blue line) with  $\alpha = 5.328 \times 10^{-4}$  and  $\xi = 7.629 \times 10^{-6}$ . For all the plasma electrons with spin up states (green circles) the associated function  $g(b_0)$  is fitted (magenta line) with  $\eta = 5.753 \times 10^{-4}$  and  $\delta = -7.615 \times 10^{-6}$ . For the mixed electron species present in plasma (black line) nicely coincides with the classical results (black open circles) with  $\mu_B = 0$ .

Ref. [27]) the scaling with the magnetic field for  $\omega \ll \omega_c$  is

$$n_+ - n_- \propto B_0^{-1}$$

which is confirmed in Fig. 6 to a very good accuracy.

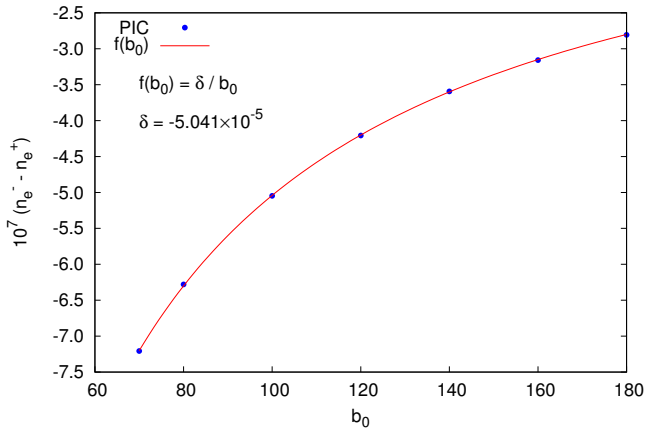


FIG. 6. The magnetization as a function of applied magnetic field (blue circles) is fitted with function  $f(b_0)$  (red line).

Extensions of PIC-codes to include the spin effects can be particularly relevant for ICF plasmas. As demonstrated by Ref. [26], the spin dependent part of the ponderomotive force can give raise to significant spin polarization for plasmas with metallic densities and higher, provided the pulse length is not too short (cf Eq. (24) of Ref. [26]) Furthermore, the generation of strong quasi-static magnetic field in laser-plasma interaction, even approaching giga-gauss values [30], means that

the background plasma can be significantly spin-polarized, since  $\mu_B B / k_B T$  can approach unity in the fast ignition scenario where the compression takes place before the heating [31]. In the present study we have focused on validating validate the code against the theoretical results of Ref. [27], and hence picked parameter values corresponding to astrophysical regimes. By comparing with analytical theory we have verified that the code executes properly and with good accuracy. In particular, studying the effects of a weakly modulated high-frequency pulse, it has been shown that the low-frequency wake-field is modified by the magnetic dipole force as predicted by theory (in particular, see Fig. 5). Furthermore, the spin polarization induced by the high-frequency wave in an system that initially is not spin-polarized agrees well with theory (see Fig. 6). This paper should be considered as a first step towards a full spin PIC-code. Besides generalizing the code to higher dimensions, it would be of much interest to include the spin dynamics (e.g. spin precession), in which case it would be possible to resolve the dynamics on the high-frequency cyclotron scale.

\* E-mail address: gert.brodin@physics.umu.se

† E-mail address: amol.holkundkar@physics.umu.se; Currently at: Department of Physics, Birla Institute of Technology and Science, Pilani, Rajasthan 333 031, India. (amol.holkundkar@bits-pilani.ac.in)

‡ E-mail address: mattias.marklund@physics.umu.se; Also at: Department of Applied Physics, Chalmers University of Technology, SE-412 96 Göteborg, Sweden

- [1] M. Bonitz, *Quantum Kinetic Theory*, (B.G. Teubner, Stuttgart, Leipzig, 1998).
- [2] G. Manfredi, *Fields Inst. Commun.* **46**, 263 (2005).
- [3] S. H. Glenzer and R. Redmer, *Rev. Mod. Phys.* **81**, 1625 (2009).
- [4] P. K. Shukla and B. Eliasson, *Physics Uspekhi* **53**, 51 (2010).
- [5] P. K. Shukla and B. Eliasson, *Rev. Mod. Phys.* **83**, 885 (2011).
- [6] H. A. Atwater, *Sci. Am.* **296**, 56 (2007).
- [7] M. Marklund, G. Brodin, L. Stenflo, and C. S. Liu, *Europhys. Lett.* **84**, 17006 (2008).
- [8] G. Manfredi and P.-A. Hervieux, *Appl. Phys. Lett.* **91**, 061108 (2007).
- [9] S. H. Glenzer *et al.*, *Phys. Rev. Lett.* **98**, 065002 (2007).
- [10] A. K. Harding and D. Lai, *Rep. Prog. Phys.* **69**, 2631 (2006).
- [11] F. Haas, *Phys. Plasmas* **12**, 062117 (2005).
- [12] F. Haas, M. Marklund and G. Brodin and J. Zamanian, *Phys. Lett A.* **374**, 481 (2010)
- [13] F. Haas, J. Zamanian, M. Marklund and G. Brodin, *New J. Phys.* **12**, 073027 (2010).
- [14] P. K. Shukla, *Nature Phys.* **5**, 92 - 93 (2009)
- [15] G. Brodin M. Marklund and G. Manfredi, *Phys. Rev. Lett.* **100**, 175001 (2008).
- [16] J. Zamanian, M. Marklund and G. Brodin, *New J. Phys.* **12**, 043019 (2010).
- [17] F. A. Asenjo, J. Zamanian1, M. Marklund, G. Brodin and P. Johansson, *New J. Phys.* **14**, 073042 (2011).
- [18] J. Dawson, *Rev. Mod. Phys.* **55**, 403 (1983).
- [19] A. Pukhov and J. Meyer-ter-Vehn, *Phys. Rev. Lett.* **76**, (1996).
- [20] A. Pukhov and J. Meyer-ter-Vehn, *Appl. Phys. B* **74**, 355 (2002)
- [21] R. Lichters, R. E. W. Pfund, and J. Meyer-Ter-Vehn,

- LPIC++: A parallel one-dimensional relativistic electromagnetic particle-in-cell-code for simulating laser-plasma-interactions*, **Report MPQ 225**, (the code is available at <http://www.lichters.net/download.html>)
- [22] J. Tonge, D.E. Dauger and V.K. Decyk, *Comp. Phys. Commun.*, **164**, 279 (2004) .
  - [23] D. E. Dauger, V. K. Decyk and J. M. Dawson, *J. Comp. Phys.*, **209** 559 (2005).
  - [24] J. Lundin, J. Zamanian, M. Marklund, and G. Brodin, *Phys. Plasmas* **14**, 062112 (2007).
  - [25] G Brodin1, J Lundin, J Zamanian and M Stefan, *New J. Phys.* **13**, 083017 (2011).
  - [26] G. Brodin, A. P. Misra, and M. Marklund, *Phys. Rev. Lett.* **105**, 105004 (2010).
  - [27] A. P. Misra, G. Brodin, M. Marklund, and P. K. Shukla, *Phys. Plasmas* **17**, 122306 (2010).
  - [28] J. Lundin and G. Brodin, *Phys. Rev. E*, **82**, 056407 (2010).
  - [29] J. Zamanian, M. Stefan, M. Marklund and Gert Brodin, *Phys. Plasmas* **17**, 102109 (2010).
  - [30] E.L. Lindman, *HEDP*, **6**, 227 (2010); U. Wagner *et al.*, *Phys. Rev. E*, 70, 026401 (2004).
  - [31] M. Tabak, *et al.*, *Phys. Plasmas*, 1, 1626 (1994).